An Experimental and Computational Investigation Rules Out Direct Nucleophilic Addition on the N2 Ligand in Manganese Dinitrogen Complex [Cp(CO)2Mn(N2)]

Quentin Le Dé, Amal Bouammali, Christian Bijani, Laure Vendier, Iker Del rosal, Dmitry A. Valyaev, Chiara Dinoi, Antoine Simonneau

An Experimental and Computational Investigation Rules Out Direct Nucleophilic Addition on the N_2 Ligand in Manganese Dinitrogen Complex $[Cp(CO)_2Mn(N_2)]$

Quentin Le Dé,[a] Amal Bouammali,[a] Christian Bijani,[a] Laure Vendier,[a] Iker del Rosal,[b] Dmitry A. Valyaev,*[a] Chiara Dinoi*[b] and Antoine Simonneau*[a]

[a] Dr. Q. Le Dé, Dr. A. Bouammali, Dr. C. Bijani, Dr. L. Vendier, Dr. D A. Valyaev, Dr. A. Simonneau
LCC-CNRS,
Université de Toulouse, CNRS, UPS
205 route de Narbonne, BP44099, F-31077 Toulouse cedex 4, France
E-mail: dmitry.valyaev@lcc-toulouse.fr, antoine.simonneau@lcc-toulouse.fr

[b] Dr. I. del Rosal, Dr. C. Dinoi
LPCNO
CNRS & INSA, Université Paul Sabatier
135 Avenue de Rangueil, 31077 Toulouse, France

Abstract: We have re-examined the reactivity of the manganese dinitrogen complex $[Cp(CO)_2Mn(N_2)]$ (**1**, Cp = η^5-cyclopentadienyl, C_5H_5) with phenylithium (PhLi). By combining experiment and density functional theory (DFT), we have found that, unlike previously reported, the direct nucleophilic attack of the carbanion onto coordinated dinitrogen does not occur. Instead, PhLi reacts with one of the CO ligand to provide an anionic acylcarbonyl dinitrogen metallate $[Cp(CO)(N_2)MnCOPh]Li$ (**3**) that is stable only below –40 °C. Full characterization of **3** (including single crystal X-ray diffraction) was performed. This complex decomposes quickly above –20 °C with N_2 loss to give a phenylate complex $[Cp(CO)_2MnPh]Li$ (**2**). The latter compound was erroneously formulated as an anionic diazenido compound $[Cp(CO)_2MnN(Ph)=N]Li$ in earlier reports, ruling out the claimed and so-far unique behavior of the N_2 ligand in **1**. DFT calculations were run to explore both the hypothesized and the experimentally verified reactivity of **1** with PhLi and are fully consistent with our results. Direct attack of a nucleophile on metal-coordinated N_2 remains to be demonstrated.

Introduction

Nitrogen is a life-sustaining element primarily sourced from widely available, inexhaustible but commonly non-bioavailable dinitrogen. In Nature, microorganisms that express the nitrogenase metallo-enzyme distribute nitrogen to the biosphere through ammonia synthesis.[1] The discovery of the Haber-Bosch process has provided mankind with a controllable and large-scale industrial synthesis of ammonia from atmospheric nitrogen.[2] Whereas more than three quarters of the ammonia produced in Haber-Bosch plants is destined to the fertilizer market,[3] the remaining part is at the origin of every nitrogen atom found in industrially produced organic or inorganic chemicals. Consequently, as underlined by Chirik and colleagues,[4] there is motivation to extend anthropic nitrogen fixation beyond ammonia, to potentially circumvent the Haber-Bosch process and its associated CO_2 emissions. From this perspective, molecular complexes have proven to be tools of choice to functionalize dinitrogen.[4,5] By activating N_2, they can catalyze the syntheses of ammonia[6] and inorganic amines through the addition of reactive main group species.[7,8] As for the synthesis of organo-nitrogen compounds, homogeneous catalytic processes are scarce,[9,10] notwithstanding that a large number of N_2 complexes undergo C–N bond formation upon treatment with organic reagents.[4,11] Most of these transformations usually occurs by the reaction of the N_2 ligand with an electrophile: organic halides or pseudohalides react typically with terminal (**I**) or bridged bimetallic dinitrogen complexes (**II**) or N_2-derived nitrides[12] (**III**) to form diazenido,[13] hydrazido,[13g,14] hydrazonato[13f] or imido[15] species (Scheme 1, top-left).

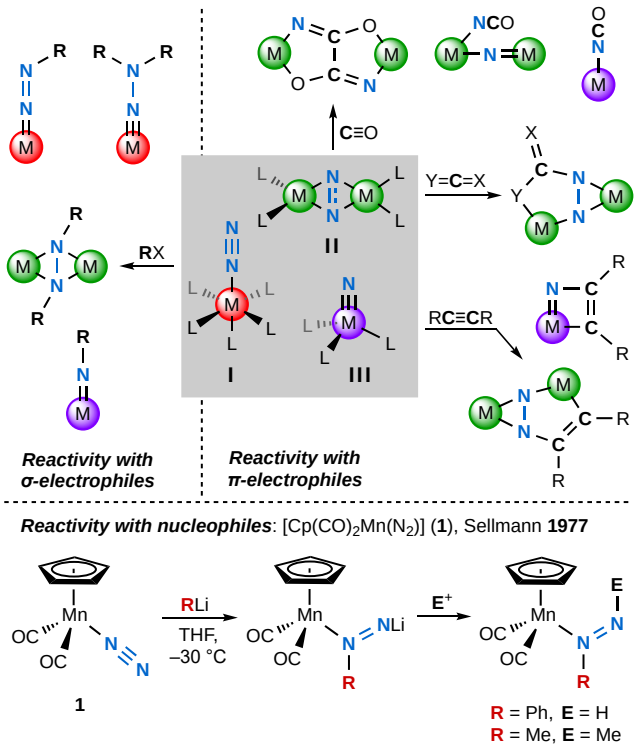

Scheme 1. Reactivity of N_2 complexes (**I**-**II**) or N_2-derived nitrides (**III**) with σ- (top-left) or π-electrophiles (top-right) vs. the unique example of nucleophilic attack on the N_2 ligand of $[Cp(CO)_2Mn(N_2)]$ (**1**) (bottom).

These C–N bonds formation methods were exploited for the synthesis of N_2-sourced amine,[16] amide,[17] hydrazine[13f,14c] or nitrile derivatives,[15,18] or the cyanate ion.[10] Early transition metal bimetallic N_2 complexes or N_2-derived nitrides can also mediate C–N bond formation with unsaturated, π-accepting (hetero)cumulenes,[19] carbon monoxide,[19d,20] isocyanides[19d,20f] or alkynes and allenes,[19d,e,21] by taking advantage of a reactive M–N linkage (Scheme 1, top-right). These latter approaches have served as a starting point for the syntheses of hydrazines,[14c,19b,e,22] amides,[20a-c] nitriles[21c] or cyanates.[19f,20a,f] An N_2 unit may also insert into a reactive M–C bond,[9,23] and the transmetallation of N_2-derived nitrides with organylpalladium species can also lead to the formation of amines (not shown).[24]

Standing in sharp contrast with those well-documented reactivity patterns, the half-sandwich Mn(I) N_2 complex $[Cp(CO)_2Mn(N_2)]$ (**1**, Cp = cyclopentadienyl, C_5H_5), described by Sellmann in the 1970s,[25] is the sole N_2 complex that was reported to mediate C–N bond formation by the addition of nucleophiles (Scheme 1, bottom). It was proposed that **1** reacts with methyl- or phenyllithium to provide an anionic α-substituted alkyl- or aryldiazenido complex $[Cp(CO)_2MnN(R)=N]Li$ (R = Me or Ph), that can be subsequently trapped with an electrophile to afford diazene products.[26] A synthetic cycle by which the diazene compound is liberated and the starting N_2 complex **1** regenerated could eventually be achieved.[26b] Such reactivity obviously recalls the well-known nucleophilic attack of RLi on a CO ligand leading to Fischer carbenes.[27] It is therefore quite intriguing that the main detectable product in the reaction of **1** with RLi was not the nucleophilic attack on CO, as observed in the reaction of cymantrene $[CpMn(CO)_3]$ with MeLi or PhLi.[28] Interested in the synthetic potential offered by the addition of polar organometallic reagents to N_2, our group has recently explored the reactivity of molybdenum and tungsten N_2 complexes with organolithium reagents, and we could not observe any N_2 functionalization.[29] Hoping a better understanding of the peculiar behavior of **1** would help delineate factors that may lead to the productive reaction of dinitrogen with polar organometallic reagents, we embarked on a re-examination of the reactivity of Sellmann's complex with PhLi using a combination of modern spectroscopic and theoretical methods. This led us to revise the initial mechanistic proposal and rule out PhLi addition on **1**'s N_2 ligand.

Results and Discussion

Synthesis and Additional Characterization of 1

The complex $[Cp(CO)_2Mn(N_2)]$ (**1**) is, to the best of our knowledge, the only isolated example of a piano-stool, terminal manganese N_2 complex.[30] It was initially prepared according to two different protocols: 1) oxidation of the hydrazine complex $[Cp(CO)_2Mn(N_2H_4)]$ by hydrogen peroxide in the presence of copper salts[25] or 2) photolysis of cymantrene in THF under N_2 pressure.[31-33] Because **1** is more conveniently isolated when the first method is employed, this is the one we have selected for this study. However, the lack of experimental details for the synthesis of **1** urged us to fully re-optimize the overall synthetic sequence (see the Supporting Information). The instability of $[Cp(CO)_2Mn(N_2H_4)]$ in the solid state even at –40 °C led us to privilege its preparation for immediate use. In order to avoid the frequent need of a photochemical set-up, we synthesized it by thermal ligand exchange from readily available $[Cp(CO)_2Mn(MeCN)]$[34] (Scheme 2). For the last step, we found that 0.3 equiv. of $Cu(OTf)_2$ and 2.1 equiv. of H_2O_2 provided the best spectroscopic yields of **1**. After evaporation of the volatiles and sublimation, **1** was recovered with reproducible yields of around 30%.

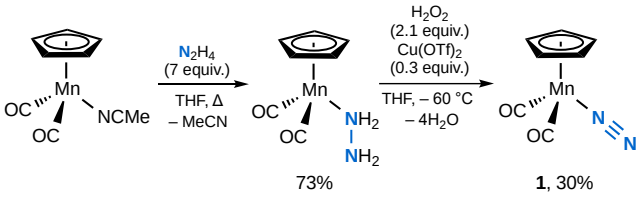

Scheme 2. Synthesis of $[Cp(CO)_2Mn(N_2)]$ (**1**).

Complex **1** is labile in solution above –10 °C, especially in polar, coordinating solvents. It was found moderately stable in the solid state, with increasing amounts of cymantrene building up over weeks at –40 °C, as evidenced by IR spectroscopy. It cannot be separated from cymantrene, the main side-product in the synthesis of **1**.[35] Trace amount is found in the NMR spectra or evidenced by the observation of weakly intense ν_{CO} stretching bands along those of **1** in the IR spectrum (THF) of the sublimed product. Complex **1** is characterized in the group frequency region by three intense bands at 2162, 1965 and 1910 cm^{-1} corresponding to N≡N, symmetric (A') and antisymmetric (A") C≡O stretches, respectively. By comparison, cymantrene exhibits bands at 2021 and 1932 cm^{-1}, resulting from symmetric and two degenerate antisymmetric C≡O stretches. Elemental analyses have allowed us to estimate the content of cymantrene to about 7–10% depending on the sample. The material condensing on the cold finger of the sublimation apparatus was suitable for a single crystal X-ray diffraction (sc-XRD) study, allowing us to get the so-far unreported solid-state structure of this organometallic N_2 complex (Figure 1). It crystallizes in the monoclinic crystal system and its space group is $P2_1/n$. The two CO ligands are eclipsed with C–H bonds of the Cp ligand. The N–N bond is 1.1144(1) Å, typical of a weakly activated N_2 ligand, and the Mn–N bond is 1.8418(4) Å, close to those reported for dinuclear μ-η^1:η^1 Mn(I)-N_2 complexes,[36] but longer than the one found in $[Mn(H)(N_2)(dmpe)_2]$ (1.817(5) Å).[37] Compared to a recent high-resolution X-ray structure of cymantrene,[38] **1** shares the same crystal system and space group. The distances between Mn and the Cp centroids are comparable (1.77 Å), but the C–C bonds of the Cp rings in **1** are sensibly shorter (avg. 1.409[4] Å) than in cymantrene (avg. 1.423[1] Å), probably as a result of a less pronounced N_2 trans influence.[39] In the considered structure of cymantrene, Mn–CO and C–O bond lengths are equal, but slight differences are observed in the structure of **1**, which can be explained by the fact that they do not exhibit the same number of short C_{Cp}–H···O contacts in the lattice (Figure S31).[40]

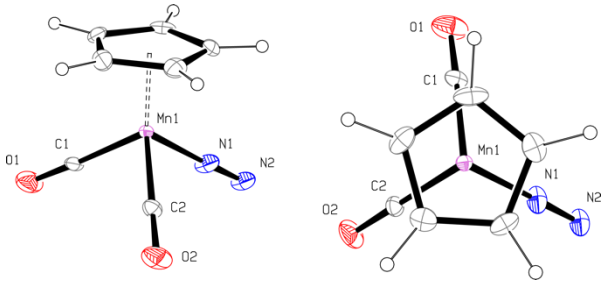

Figure 1. Solid-state molecular structure of 1 along two projections. Thermal ellipsoids at the 30% probability level. Selected bond lengths (Å): Mn1-N1 1.8418(4), N1-N2 1.1144(1), Mn1-C1 1.822(3), Mn1-C2 1.795(3), C1-O1 1.128(4), C2-O2 1.142(4).

Reaction of 1 with PhLi: Spectroscopic Monitoring

With complex **1** in hand, we next checked its reactivity with phenyllithium.[26a] Real-time IR spectroscopy was found to be an analytical method of choice to monitor the progress of this reaction (Figure 2A,B and Figure S25). Treatment of **1** with PhLi in THF at ca. –40 °C led, after 1.5 h, to a product **2** that had the same IR signature as the species reported by Sellmann, assigned to the anionic diazenido complex $[Cp(CO)_2MnN(Ph)=N]Li$. Complex **2** was characterized by three CO stretching bands at 1869, 1792 and 1755 cm^{-1}, shifted towards lower frequencies compared to **1**. The observation of a third band was attributed to a possible equilibrium between the associated and solvent-separated ion pair.[41] In agreement with this hypothesis, addition of 12-*c*-4 at the end of the experiment resulted in the immediate disappearance of the 1756 cm^{-1} band, leaving in the spectrum those of the unperturbed anion (Figure 2B). Interestingly, during the initial stage of the reaction (first 30 min), a compound **3** featuring rather intense bands at 2044 and 1840 cm^{-1}, was detected. Noteworthy, these spectral features were absent from Sellmann's original reports, and IR data for this species are consistent with an anionic end-on N_2 complex having only one carbonyl ligand, possibly playing a key role in the overall reaction. Importantly, at lower temperature (ca. –50 °C), the reaction of **1** with PhLi led exclusively to **3** and its evolution toward **2** was found very slow (Figure S26), but above –20 °C this transformation proceeded quickly. Having established the stability of **3** in solution at low temperature, we attempted to characterize it by NMR. Adding **1** to a cooled (–78 °C) THF-d_8 solution of PhLi and introduction of the sample into an NMR spectrometer stabilized at –50 °C allowed us to gain additional information on the nature of **3**. Indeed, the $^{13}C\{^1H\}$ spectrum showed a singlet at δ_C 318.0 ppm, accompanied by the expected CO, Cp and aromatic carbon resonances (see Figures 2D and S28-29). A correlation was found between aromatic protons and the low field signal using a ^1H-^{13}C HMBC-NMR experiment. Collectively, these data point to an anionic acylcarbonyl metallate formulation for **3**.[42] Upon warming up of the probe to –40 °C, characteristic resonances of **3** disappeared over 24 h. A new major compound built up that did not feature any carbon resonance at higher field than the CO signals, along with minor amounts of the anionic acylcarbonyl metallate $[Cp(CO)_2MnCOPh]Li$ (**4**). An IR measurement on the resulting THF-d_8 solution confirmed that the major final product had the same spectrum as **2**.

Isolation and Structure of the Observed Species

We next considered the isolation and crystallization of **2** and **3**. Because of the good solubility of both **2** and **3** in THF, as well as the thermal and vacuum sensitivity of **3**, we attempted the reaction of **1** with phenyllithium in the less polar solvent Et_2O, hoping it would facilitate crystallization. However, no reaction occurred. Reasoning that the lack of reactivity could be attributed to the equilibrated tetrameric/dimeric nature of PhLi in Et_2O, we added PMDTA (*N*,*N*,*N'*,*N'*,*N''*-pentamethyldiethylenetriamine) to convert it into monomeric PhLi·PMDTA (Scheme 3).[43] To our delight, immediate reactivity was observed according to IR monitoring, **3**·PMDTA being observed at low temperature.[44] By layering the reaction mixture with pentane, we managed to obtain crystals suitable for an sc-XRD analysis that allowed confirmation of the proposed structure for **3** (Figure 3, left). In agreement with the lower frequency of the N≡N stretch recorded for **3** by comparison with **1**, the N–N bond length is longer in the former compound (1.138[6][45] *vs*. 1.1144[1] Å for **1**). To lift any ambiguity arising from discrimination between N_2 and CO during structure resolution, we have also prepared and crystallized $[Cp(CO)_2MnCOPh][Li(PMDTA)]$ (**4**·PMDTA) (Figure 3, middle) from cymantrene to ascertain the structure of **3**·PMDTA is the one of a genuine dinitrogen complex. Compound **4**·PMDTA crystallizes in a different space group than **3**·PMDTA, with C–O bonds measuring 1.175(4) and 1.179(4) Å, significantly longer than the N–N bond length in **3**·PMDTA (1.138[6] Å). Beyond these disparities, the two structures are rather similar and variations in bond lengths do not exceed 0.03 Å. The lithium ion binds to the acyl's oxygen, and establishes short contacts with a remote N_2 (**3**·PMDTA) or CO (**4**·PMDTA) ligand. At the macroscopic scale, a striking difference between crystals of **3**·PMDTA and **4**·PMDTA was that the former visibly evolved gaseous N_2 upon warming to RT.

Compound **3**·PMDTA in solution is also sensitive to temperature and vacuum, like unsupported **3**, and rearranged into **2**·PMDTA in solution above –20 °C according to IR spectroscopy. Signs of decomposition were also evidenced for crystals of **3**·PMDTA over few days at –40 °C. Complex **2**·PMDTA could be crystallized in similar conditions than for **3**·PMDTA. To our surprise, the sc-XRD analysis revealed that **2**·PMDTA was not the proposed anionic diazenido complex but a rare example of Mn(I) phenylmanganate compound,[46] $[Cp(CO)_2MnPh]Li$·PMDTA (Figure 3, right). This result indeed pointed to a wrong assignment of the structure of **2**, since spectroscopic data of the PMDTA adduct were found very close to those of **2** recorded under Sellmann's conditions (Figures 2C, S20-21 and S28-29).

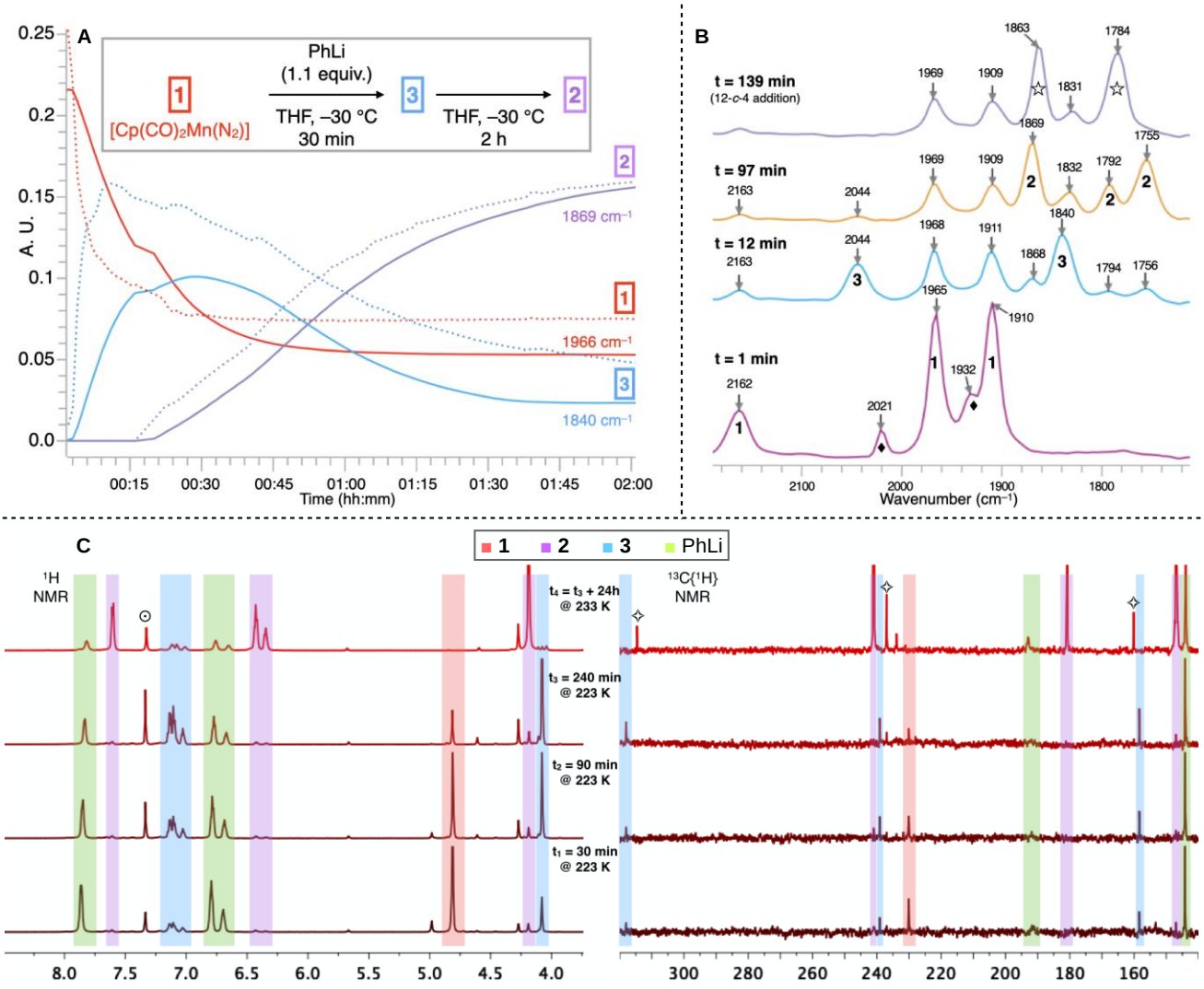

Figure 2. A) Smoothed (plain lines) and raw (dotted lines) kinetic plots of the reaction of $[Cp(CO)_2Mn(N_2)]$ (**1**) with PhLi (1.1 equiv., THF, ca. –30 °C) showing the absorbance of the most intense CO stretching band of the three main species detected by real-time IR monitoring. B) IR spectra recorded at different times of the reaction. ♦□ $[CpMn(CO)_3]$ present in the starting material; ☆ **2**, separated ion pair. C) Stacked spectra of ^{1}H- (left, 600 MHz) and $^{13}C\{^1H\}$-NMR (right, 150 MHz) monitoring in THF-d_8 at low temperature focusing on the Cp/aromatic and carbonyl regions, respectively. ⊙ C_6H_6; ✧ $[Cp(CO)_2MnCOPh]Li$ (**4**).

Yet, to confirm that the change of reaction medium and the presence of the polyamine was not influencing the outcome of this reaction, we decided to carry out an independent synthesis of $[Cp(CO)_2MnPh]Li$ (**2**) in THF in order to compare its spectral signature to the product obtained in the original Sellmann's conditions. Although being a rather simple organometallic species, no preparative method was reported for **2**. The reaction of photo-generated $[Cp(CO)_2Mn(THF)]$ with PhLi in THF at low temperature led to a mixture of compounds, and most of them decomposed upon isolation attempts. We next wondered whether $[Cp(CO)_2MnCOPh]Li$ (**4**) could not produce **2** upon photo-decarbonylation.[48] Gratifyingly, irradiation of a THF solution of **4**, obtained by reacting PhLi with cymantrene,[28] cleanly led to the formation of the -ate complex **2** (Scheme 4). Spectral match (IR and NMR, compare Figures S16-17 and S28-29) with the supposed anionic diazenido compound was noted, pointing conclusively to a misassignment of the structure of product **2**. It corresponds *de facto* to the phenylate complex $[Cp(CO)_2MnPh]Li$, which no longer incorporates N_2 and originates from the degradation of **3**, which is rapid when the latter is exposed to temperatures higher than –20 °C (Scheme 3).[49]

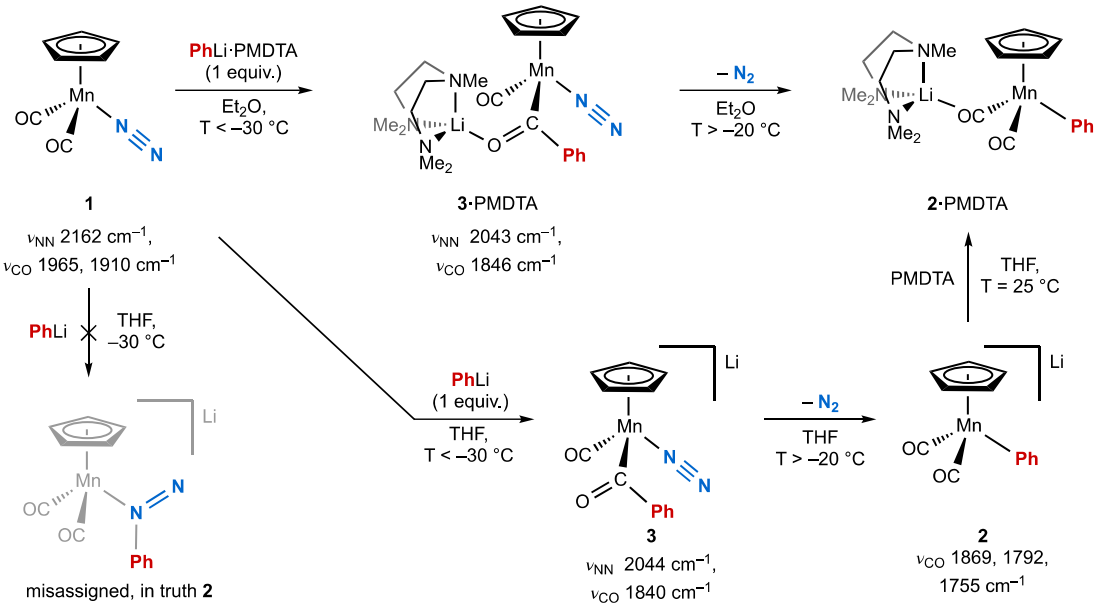

Scheme 3. Overview of the reactivity of **1** with PhLi. Infrared stretching frequencies from *in situ* measurements.

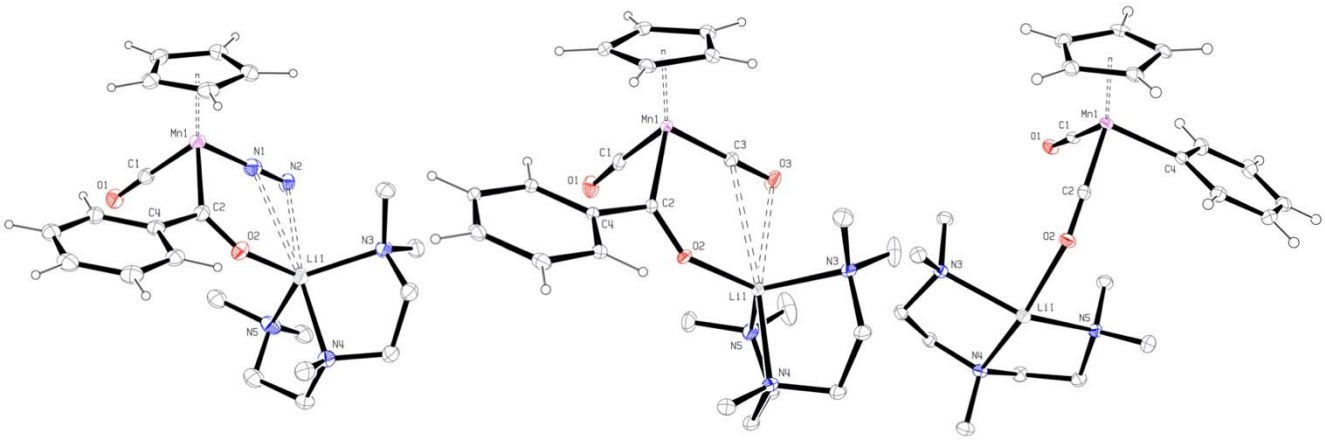

Figure 3. Solid-state molecular structures of **3**·PMDTA (left), **4**·PMDTA (middle) and polymeric **2**·PMDTA (right),[47] with thermal ellipsoids set at the 20% (**3**·PMDTA, **4**·PMDTA) and 30% (**2**·PMDTA) probability levels. For clarity, hydrogen atoms of the PMDTA ligands have been omitted and only one disordered component of the triamine moiety is shown. In both structures, the short contacts ($d < \Sigma r_{vdW}$) between the lithium ion and a remote ligand are represented with dashed lines. Selected bond lengths (Å) for **3**·PMDTA: Mn1-N1 1.800(4), Mn1-C1 1.769(4), Mn1-C2 1.964(4), N1-N2 1.138(6), C1-O1 1.163(5), C2-O2 1.243(5), C2-C4 1.517(6), O2-Li1 1.843(8). For **4**·PMDTA: Mn1-C1 1.745(3), Mn1-C2 1.958(3), Mn1-C3 1.758(4), C1-O1 1.175(4), C2-O2 1.256(3), C3-O3 1.179(4), C2-C4 1.518(4), O2-Li1 1.864(5). For **2**·PMDTA: Mn1-C1 1.7367(15), Mn1-C2 1.7446(15), Mn1-C4 2.0430(15), C1-O1 1.1852(18), C2-O2 1.1860(18), O1-Li1 1.969(3), O1···Li1 2.208(3).

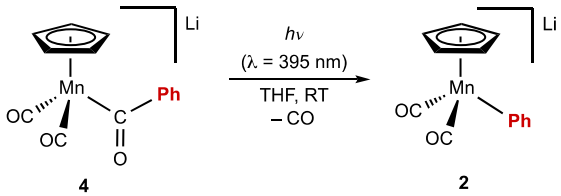

Scheme 4. Photochemical synthesis of the phenyl manganate complex **2**.

DFT Calculations

The reaction of **1** with PhLi in THF was explored with DFT at the B3PW91 level of theory to verify whether our experimental findings would be supported *in silico*. The optimized structure of **1** (**1**$_{opt}$) is shown in Figure S36. Calculated bond distances and angles as well as representative ^{1}H and ^{13}C NMR chemical shifts are listed in Table 1 and compared with those experimentally observed. The computed bond distances and angles accurately reproduce the values obtained experimentally with variations of less than 0.04 Å. The disparities of C–O and Mn–CO bond lengths in the experimental structure of **1** were indeed not found in the computed structure since they were the result of intermolecular short contacts within the crystal lattice. The IR stretching frequencies for the N–N and C–O bonds were calculated[50] at 2191 and 1974 (A'), 1934 cm^{-1} (A"), respectively, and correspond well to the measured values (2162 and 1965, 1910 cm^{-1}). The most representative ^{1}H and ^{13}C chemical shifts also show a good

agreement between theory and experiment. In order to evaluate the effect of the coordination to the Mn center on the polarization of the CO and N_2 ligands, we computed the natural charges of **1** *via* a NBO analysis (Figure S37). Compared to free CO, which displays a positive and negative charge of +0.50 and -0.50 at the C and O atoms, respectively, the Mn coordinated CO ligand carries an identical natural charge at oxygen (-0.48) but a more positive natural charge (+0.86) at carbon, reflecting the higher CO polarization after coordination. On the other hand, while the coordination of N_2 to manganese leaves the charge of the β nitrogen unchanged (0.0), it slightly increases the charge of the α nitrogen (from 0.0 to 0.18), pointing to a lower polarization of the N_2 bond compared to the CO one. Therefore, in complex **1**, the most positive charge is localized on the C atoms of the CO ligands, indicating that their electrophilicity overcomes that of both the α and β nitrogen atoms of the N_2 ligand.

Table 1. Comparison of representative bond lengths (Å), angles (°) and chemical shifts (ppm) obtained experimentally by sc-XRD and NMR analyses on **1**, with those of the DFT-optimized $\mathbf{1}_{opt}$.

Complex	**1**	$\mathbf{1}_{opt}$
N≡N	1.1144(1)	1.119
C≡O	1.128(4), 1.142(4)	1.160
Mn–CO	1.822(3), 1.795(3)	1.775, 1.776
Mn–N	1.8418(4)	1.835
Mn–C_{Cp}	2.137(3)[a]	2.150
Mn−N−N	178.44	177.7
δ_H Cp	4.87	4.79
δ_C Cp	83.0	85.0
δ_C CO	229.0	230.8

[a] averaged metrical data

In order to rationalize the formation of complexes **3** and **2** we focused on the mechanism involved in the reaction between **1** and phenyllithium in THF. Three mechanistic pathways have been computed, involving the direct nucleophilic attack of phenyllithium onto i) the carbon of one of the carbonyl ligands of **1**; ii) the proximal (α) nitrogen and iii) the distal (β) nitrogen of the dinitrogen ligand of **1** (Figure 4, variations of the computational parameters can be found in Figures S39–43). The formation of the α-phenyldiazenido Mn complex ($\mathbf{5}_{opt}$) is an endothermic reaction (ΔH = 9.3 kcal/mol), passing through a transition state, $\mathbf{TS_{1\rightarrow5}^{\alpha}}$, located at ΔH = 23.1 kcal/mol. This transition state is prepared by a local minimum adduct ($\mathbf{Int_{1\rightarrow TS}^{\alpha}}$ at 16.2 kcal/mol) in which the Ph anion is not anymore coordinated to the Li center and the $Li(THF)_3$ cation interacts with the N_2 ligand of the $[CpMn(CO)_2(N_2)]$ complex. The nucleophilic attack of phenyl lithium onto the β (distal) nitrogen has an identical kinetic barrier (ΔH = 22.9 kcal/mol), although the formation of the resulting β-phenyldiazenido Mn complex ($\mathbf{5}^{\beta}_{opt}$) is computed to be an athermic process (ΔH = 0.0 kcal/mol). On the other hand, the addition of PhLi onto one of the carbonyl ligands of **1** involves a low energy transition state ($\mathbf{TS_{1\rightarrow3}}$, ΔH = 12.7 kcal/mol), affording the σ-acyl dinitrogen complex ($\mathbf{3}_{opt}$) by a highly exothermic process (ΔH = –25.6 kcal/mol). In accordance with the experimental results, these three computed profiles clearly show that the nucleophilic attack of the carbanion on the carbonyl's carbon is favored over those on nitrogen from both a kinetic and thermodynamic point of view. The acylcarbonyl dinitrogen metallate $[Cp(CO)(N_2)MnCOPh]Li$ (**3**) is therefore the only possible product of the reaction between **1** and phenyllithium below –30 °C. The computed structures for $\mathbf{3}_{opt}$ and $\mathbf{3}\cdot PMDTA_{opt}$, containing respectively the $Li(THF)_3^+$ and $Li(PMDTA)^+$ cations, are shown in Figure S38. Their most representative distances and angles accurately reproduce the values obtained experimentally (Table S6). The two computed stretching frequencies for the N≡N and C≡O bonds are 2080 and 1864 cm^{-1} for $\mathbf{3}\cdot PMDTA_{opt}$ and 2092 and 1863 cm^{-1} for $\mathbf{3}_{opt}$, respectively. They fall close to the experimental values of 2044 and 1840 cm^{-1} measured for **3** and 2043 and 1846 cm^{-1} for **3**·PMDTA (in Et_2O).

Starting from intermediate **3**, we then computed the formation of the final phenylate complex **2**, through dinitrogen dissociation. As shown in Figure 4, the formation of N_2-free $\mathbf{2}_{opt}$ can be achieved by a two-step process which involves the dissociation of N_2 to obtain the N_2-free acylcarbonyl intermediate ($\mathbf{Int_{3\rightarrow2}}$) followed, at a later stage, by the metallation of the aromatic ring. The two kinetic barriers involved in this process lie 23.5 ($\mathbf{TS_{3\rightarrow Int}}$) and 21.2 ($\mathbf{TS_{Int\rightarrow2}}$) kcal/mol above $\mathbf{3}_{opt}$, making the process feasible at temperatures above –20 °C. Although the formation of $\mathbf{2}_{opt}$ is nearly athermal, the loss of dinitrogen in solution is likely to drive the equilibrium towards the phenylate complex. Finally, a pathway connecting the σ-acyl dinitrogen metallate $\mathbf{3}_{opt}$ with the anionic phenyldiazenido complex $\mathbf{5}_{opt}$ could be computed (Figure 4, orange profile). Phenyl transfer from the carbonyl to the dinitrogen ligand occurs *via* a C-to-N 1,3-sigmatropic shift at a very high energetic cost ($\mathbf{TS_{3\rightarrow5}^{\alpha}}$, ΔH = 70.8 kcal/mol, with an associated kinetic barrier of 96.4 kcal/mol relative to $\mathbf{3}_{opt}$), making this elementary step improbable under the actual experimental conditions and surely not competitive with the formation of **2**. Calculated values for representative ^1H and ^{13}C NMR chemical shifts, as well as C≡O stretching frequencies for $\mathbf{2}_{opt}$ were indeed found closer to the experimentally recorded ones (Figure 2) than those computed for $\mathbf{5}_{opt}$ (Table S7).

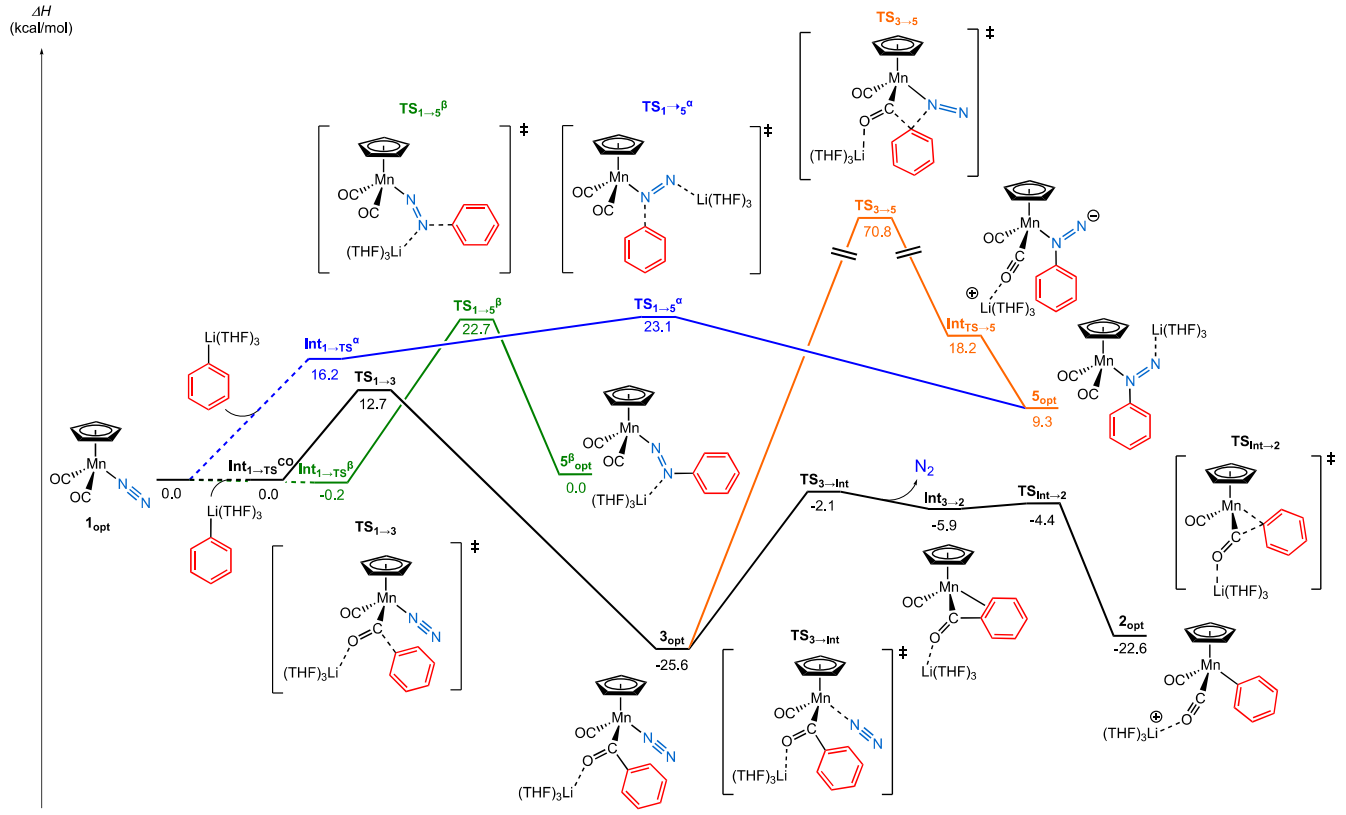

Figure 4. Enthalpy profiles at the B3PW91/SMD level of theory (6-31G** for C, N, O, H, 6-311++G** for Li and SDDALL for Mn) for hypothesized and experimentally verified reactivity for $[Cp(CO)_2Mn(N_2)]$ (**1**). Black: enthalpy profile of the experimentally observed pathway consisting of a first nucleophilic attack of $PhLi(THF)_3$ onto one of the CO ligands of **1** leading to $\mathbf{3}_{opt}$, followed by N_2 loss and metalation of the aromatic group to give $\mathbf{2}_{opt}$. Blue: enthalpy profile of the previously proposed reactivity for **1** where $PhLi(THF)_3$ attacks the proximal (α) nitrogen of the N_2 ligand, leading to $\mathbf{5}_{opt}$. Green: enthalpy profile of an alternative, hypothetical nucleophilic attack of $PhLi(THF)_3$ onto the distal (β) nitrogen of the N_2 ligand. Orange: calculated pathway connecting $\mathbf{3}_{opt}$ to $\mathbf{5}_{opt}$ *via* a C-to-N 1,3-sigmatropic shift of the phenyl group.

Conclusion

In this article, we have re-examined the previously reported reactivity of Sellmann's $[Cp(CO)_2Mn(N_2)]$ complex (**1**) towards phenyllithium and additionally report its so-far missing structure. Combining experiment and theory, we have found that, contrary to what was initially proposed by Sellmann, the direct attack of phenyllithium on the dinitrogen ligand in **1** to give an anionic α-phenyldiazenido Mn complex $[Cp(CO)_2MnN(Ph)=N]Li$ is unlikely. The compound observed by Sellmann with IR spectroscopy that was assigned to the latter structure is actually the phenyl manganate complex $[Cp(CO)_2MnPh]Li$ (**2**), no longer incorporating N_2. We have also discovered that at low temperature, the reaction of **1** with PhLi leads to the formation of the anionic σ-acyl dinitrogen manganate complex $[Cp(CO)(N_2)MnCOPh]Li$ (**3**) resulting from the attack of the carbanion onto one of the carbonyl ligands in **1**.[49] DFT calculations confirmed the net preference for nucleophilic attack at CO over N_2. From **3**, CO-to-N_2 phenyl transfer to give $[Cp(CO)_2MnN(Ph)=N]Li$ has been computed to be kinetically unfeasible, while a pathway has been modelled for the transformation of **3** into the phenylate complex **2**, initiated by N_2 dissociation.

How Sellmann was able to obtain diazenes from **1**[26b,c] (see Scheme 1) remains an open question. It seems unlikely that the treatment of the N_2-free phenyl metallate **2** with an electrophile would afford a diazene complex. We believe **3** may be involved in this transformation, and that it was actually the species that reacted with the electrophile in Sellmann's experiments[51] – its thermal sensitivity precluding its detection in aliquots by IR spectroscopy and leading to the observation of N_2-free **2** – under a mechanism that still has to be unveiled. Yet, our findings show that nucleophilic attack on coordinated N_2 remains to be demonstrated. The results of a combined experimental and theoretical investigation on the reactivity of **3** and **2** with electrophiles will be reported shortly.

Acknowledgements

Q. L., A. B., D. A. V. and A. S. acknowledge the European Research Council for funding (grant agreement 757501). Q. L. D., A. B., C. B., L. V., D. A. V. and A. S. would like to thank the CNRS for general support. I. d. R. and C. D. are indebted to CALMIP for HPC resources (Grant 2017-[p17010])

Keywords: dinitrogen • manganese • organolithium • carbon monoxide • cyclopentadienyl

[1] a) O. Einsle, D. C. Rees, *Chem. Rev.* **2020**, *120*, 4969–5004; b) L. C. Seefeldt, Z.-Y. Yang, D. A. Lukoyanov, D. F. Harris, D. R. Dean, S. Raugei, B. M. Hoffman, *Chem. Rev.* **2020**, *120*, 5082–5106. (c) B. M. Hoffman, D. Lukoyanov, Z.-Y. Yang, D. R. Dean, L. C. Seefeldt, *Chem. Rev.* **2014**, *114*, 4041–4062.

[2] a) M. Appl in *Ullmann's Encyclopedia of Industrial Chemistry, Vol. 3*, Wiley-VCH Verlag GmbH & Co. KGaA, Weinheim, **2011**, pp. 139–225; b) V. Smil, *Enriching the Earth: Fritz Haber, Carl Bosch, and the Transformation of World Food Production*, MIT Press, Cambridge, **2001**; c) J. R. Jennings, *Catalytic Ammonia Synthesis: Fundamentals and Practice*, Springer, New York, **1991**.

[3] M. Appl in *Ullmann's Encyclopedia of Industrial Chemistry, Vol. 3*, Wiley-VCH Verlag GmbH & Co. KGaA, Weinheim, **2011**, pp. 107–137.

[4] S. Kim, F. Loose, P. J. Chirik, *Chem. Rev.* **2020**, *120*, 5637–5681.

[5] a) F. Masero, M. A. Perrin, S. Dey, V. Mougel, *Chem. – Eur. J.* **2021**, *27*, 3892–3928; b) D. Singh, W. R. Buratto, J. F. Torres, L. J. Murray, *Chem. Rev.* **2020**, *120*, 5517–5581; c) *Transition Metal-Dinitrogen Complexes: Preparation and Reactivity* (Ed. Y. Nishibayashi), Wiley-VCH Verlag GmbH & Co. KGaA: Weinheim, **2019**; d) M. D. Walter in *Advances in Organometallic Chemistry, Vol. 65* (Ed. P. J. Pérez), Elsevier, **2016**, pp. 261–377; e) P. J. Chirik, *Dalton Trans.* **2007**, 16–25; f) S. Gambarotta, J. Scott, *Angew. Chem. Int. Ed.* **2004**, *43*, 5298–5308; g) B. A. MacKay, M. D. Fryzuk, *Chem. Rev.* **2004**, *104*, 385–402.

[6] Recent reviews: a) Y. Tanabe, Y. Nishibayashi, *Chem. Soc. Rev.* **2021**, *50*, 5201–5242; b) M. J. Chalkley, M. W. Drover, J. C. Peters, *Chem. Rev.* **2020**, *120*, 5582–5636.

[7] a) Y. Tanabe, Y. Nishibayashi, *Coord. Chem. Rev.* **2019**, *389*, 73–93; b) S. Bennaamane, M. F. Espada, A. Mulas, T. Personeni, N. Saffon-Merceron, M. Fustier-Boutignon, C. Bucher, N. Mézailles, *Angew. Chem. Int. Ed.* **2021**, *60*, 20210–20214.

[8] Borylenes and boryl radicals may react spontaneously with N_2: a) M.-A. Légaré, G. Bélanger-Chabot, R. D. Dewhurst, E. Welz, I. Krummenacher, B. Engels, H. Braunschweig, *Science* **2018**, *359*, 896–900; b) S. Bennaamane, B. Rialland, L. Khrouz, M. Fustier-Boutignon, C. Bucher, E. Clot, N. Mézailles, *Angew. Chem. Int. Ed.* **2023**, *62*, e202209102.

[9] S. F. McWilliams, D. L. J. Broere, C. J. V. Halliday, S. M. Bhutto, B. Q. Mercado, P. L. Holland, *Nature* **2020**, *584*, 221–226.

[10] T. Itabashi, K. Arashiba, A. Egi, H. Tanaka, K. Sugiyama, S. Suginome, S. Kuriyama, K. Yoshizawa, Y. Nishibayashi, *Nat. Commun.* **2022**, *13*, 6161.

[11] a) Z.-J. Lv, J. Wei, W.-X. Zhang, P. Chen, D. Deng, Z.-J. Shi, Z. Xi, *Natl. Sci. Rev.* **2020**, *7*, 1564–1583; b) M. Mori, *J. Organomet. Chem.* **2004**, *689*, 4210–4227; c) M. Hidai, Y. Mizobe, *Top. Organomet. Chem.* **1999**, *3*, 227–241.

[12] S. J. K. Forrest, B. Schluschaß, E. Y. Yuzik-Klimova, S. Schneider, *Chem. Rev.* **2021**, *121*, 6522–6587.

[13] Selected examples: a) V. W. Day, T. A. George, S. D. A. Iske, *J. Am. Chem. Soc.* **1975**, *97*, 4127–4128; b) J. Chatt, A. A. Diamantis, G. A. Heath, N. E. Hooper, G. J. Leigh, *Chem. Soc. Dalton Trans.* **1977**, 688–697; c) T. Yoshida, T. Adachi, T. Ueda, M. Kaminaka, N. Sasaki, T. Higuchi, T. Aoshima, I. Mega, Y. Mizobe, M. Hidai, *Angew. Chem. Int. Ed. Engl.* **1989**, *28*, 1040–1042; d) J. C. Peters, J.-P. F. Cherry, J. C. Thomas, L. Baraldo, D. J. Mindiola, W. M. Davis, C. C. Cummins, *J. Am. Chem. Soc.* **1999**, *121*, 10053–10067; e) M. D. Fryzuk, S. A. Johnson, B. O. Patrick, A. Albinati, S. A. Mason, T. F. Koetzle, *J. Am. Chem. Soc.* **2001**, *123*, 3960–3973; f) D. J. Knobloch, D. Benito-Garagorri, W. H. Bernskoetter, I. Keresztes, E. Lobkovsky, H. Toomey, P. J. Chirik, *J. Am. Chem. Soc.* **2009**, *131*, 14903–14912; g) T. Kupfer, R. R. Schrock, *J. Am. Chem. Soc.* **2009**, *131*, 12829–12837.

[14] Selected examples: a) G. E. Bossard, T. A. George, R. K. Lester, R. C. Tisdale, R. L. Turcotte, *Inorg. Chem.* **1985**, *24*, 1129–1132; b) J. Rittle, J. C. Peters, *J. Am. Chem. Soc.* **2016**, *138*, 4243–4248; c) Z.-J. Lv, Z. Huang, W.-X. Zhang, Z. Xi, *J. Am. Chem. Soc.* **2019**, *141*, 8773–8777.

[15] Selected examples: a) J. J. Curley, E. L. Sceats, C. C. Cummins, *J. Am. Chem. Soc.* **2006**, *128*, 14036–14037; b) J. S. Figueroa, N. A. Piro, C. R. Clough, C. C. Cummins, *J. Am. Chem. Soc.* **2006**, *128*, 940–950; c) I. Klopsch, M. Kinauer, M. Finger, C. Würtele, S. Schneider, *Angew. Chem. Int. Ed.* **2016**, *55*, 4786–4789.

[16] Selected example: P. C. Bevan, J. Chatt, G. J. Leigh, E. G. Leelamani, *J. Organomet. Chem.* **1977**, *139*, C59–C62.

[17] Selected example: H. Henderickx, G. Kwakkenbos, A. Peters, J. van der Spoel, K. de Vries, *Chem. Commun.* **2003**, 2050–2051.

[18] Selected examples: Ref. 15c; a) M. M. Guru, T. Shima, Z. Hou, *Angew. Chem. Int. Ed.* **2016**, *55*, 12316–12320; b) F. Schendzielorz, M. Finger, J. Abbenseth, C. Würtele, V. Krewald, S. Schneider, *Angew. Chem. Int. Ed.* **2019**, *58*, 830–834.

[19] Selected examples: a) W. H. Bernskoetter, A. V. Olmos, J. A. Pool, E. Lobkovsky, P. J. Chirik, *J. Am. Chem. Soc.* **2006**, *128*, 10696–10697; b) W. H. Bernskoetter, E. Lobkovsky, P. J. Chirik, *Angew. Chem. Int. Ed.* **2007**, *46*, 2858–2861; c) J. Ballmann, A. Yeo, B. O. Patrick, M. D. Fryzuk, *Angew. Chem. Int. Ed.* **2011**, *50*, 507–510; d) S. P. Semproni, P. J. Chirik, *J. Am. Chem. Soc.* **2013**, *135*, 11373–11383; e) Y. Nakanishi, Y. Ishida, H. Kawaguchi, *Angew. Chem. Int. Ed.* **2017**, *56*, 9193–9197; f) Q. Zhuo, J. Yang, Z. Mo, X. Zhou, T. Shima, Y. Luo, Z. Hou, *J. Am. Chem. Soc.* **2022**, *144*, 6972–6980.

[20] Selected examples: a) D. J. Knobloch, E. Lobkovsky, P. J. Chirik, *Nat. Chem.* **2010**, *2*, 30–35; b) D. J. Knobloch, E. Lobkovsky, P. J. Chirik, *J. Am. Chem. Soc.* **2010**, *132*, 10553–10564; c) D. J. Knobloch, E. Lobkovsky, P. J. Chirik, *J. Am. Chem. Soc.* **2010**, *132*, 15340–15350; e) D. J. Knobloch, S. P. Semproni, E. Lobkovsky, P. J. Chirik, *J. Am. Chem. Soc.* **2012**, *134*, 3377–3386; f) A. F. Cozzolino, J. S. Silvia, N. Lopez, C. C. Cummins, *Dalton Trans.* **2014**, *43*, 4639–4652; g) Y. Ishida, H. Kawaguchi, *J. Am. Chem. Soc.* **2014**, *136*, 16990–16993.

[21] Selected examples: a) L. Morello, J. B. Love, B. O. Patrick, M. D. Fryzuk, *J. Am. Chem. Soc.* **2004**, *126*, 9480–9481; b) S. P. Semproni, P. J. Chirik, *Organometallics* **2014**, *33*, 3727–3737; c) J. Song, Q. Liao, X. Hong, L. Jin, N. Mézailles, *Angew. Chem. Int. Ed.* **2021**, *60*, 12242–12247.

[22] D. J. Knobloch, H. E. Toomey, P. J. Chirik, *J. Am. Chem. Soc.* **2008**, *130*, 4248–4249.

[23] a) M. E. Volpin, V. B. Shur, R. V. Kudryavtsev, L. A. Prodayko, *Chem. Commun.* **1968**, 1038–1040; b) E. G. Berkovich, V. B. Shur, M. E. Vol'pin, B. Lorenz, S. Rummel, M. Wahren, *Chem. Ber.* **1980**, *113*, 70–78; c) V. B. Shur, E. G. Berkovich, M. E. Vol'pin, B. Lorenz, M. Wahren, *J. Organomet. Chem.* **1982**, *228*, C36–C38; d) E. G. Berkovich, V. S. Lenenko, L. I. Vyshinskaya, G. A. Vasil'eva, V. B. Shur, M. E. Vol'pin, *J.*

Organomet. Chem. **1997**, *535*, 169–173; e) S. Bhutto, R. Hooper, B. Mercado, P. L. Holland, *J. Am. Chem. Soc.* **2023**, *145*, 4626-4637.

[24] a) K. Hori, M. Mori, *J. Am. Chem. Soc.* **1998**, *120*, 7651–7652; b) K. Wang, Z.-H. Deng, S.-J. Xie, D.-D. Zhai, H.-Y. Fang, Z.-J. Shi, *Nat. Commun.* **2021**, *12*, 248.

[25] D. Sellmann, *Angew. Chem. Int. Ed. Engl.* **1971**, *10*, 919.

[26] a) D. Sellmann, W. Weiss, *Angew. Chem. Int. Ed. Engl.* **1977**, *16*, 880–881; b) D. Sellmann, W. Weiss, *Angew. Chem. Int. Ed. Engl.* **1978**, *17*, 269–270; c) D. Sellmann, W. Weiss, *J. Organomet. Chem.* **1978**, *160*, 183–196.

[27] Seminal papers: a) E. O. Fischer, A. Maasböl, *Angew. Chem. Int. Ed. Engl.* **1964**, *3*, 580–581; c) O. S. Mills, A. D. Redhouse, *Angew. Chem. Int. Ed. Engl.* **1965**, *4*, 1082. A review: c) K. H. Dötz, J. Stendel, *Chem. Rev.* **2009**, *109*, 3227–3274.

[28] E. O. Fischer, A. Maasböl, *Chem. Ber.* **1967**, *100*, 2445–2456.

[29] a) A. Bouammali, C. Bijani, L. Vendier, M. Etienne, A. Simonneau, *Eur. J. Inorg. Chem.* **2020**, 1423–1427.

[30] Selected examples of other piano-stool N_2 complexes: a) M. Hirotsu, P. P. Fontaine, A. Epshteyn, L. R. Sita, *J. Am. Chem. Soc.* **2007**, *129*, 9284–9285; b) M. Hirotsu, P. P. Fontaine, P. Y. Zavalij, L. R. Sita, *J. Am. Chem. Soc.* **2007**, *129*, 12690–12692; c) P. P. Fontaine, B. L. Yonke, P. Y. Zavalij, L. R. Sita, *J. Am. Chem. Soc.* **2010**, *132*, 12273–12285; d) Y. Sunada, T. Imaoka, H. Nagashima, *Organometallics* **2010**, *29*, 6157–6160; e) A. J. Keane, B. L. Yonke, M. Hirotsu, P. Y. Zavalij, L. R. Sita, *J. Am. Chem. Soc.* **2014**, *136*, 9906–9909; f) T. Miyazaki, H. Tanaka, Y. Tanabe, M. Yuki, K. Nakajima, K. Yoshizawa, Y. Nishibayashi, *Angew. Chem. Int. Ed.* **2014**, *53*, 11488–11492; g) Reference 18b; h) J. Yin, J. Li, G.-X. Wang, Z.-B. Yin, W.-X. Zhang, Z. Xi, *J. Am. Chem. Soc.* **2019**, *141*, 4241–4247; h) E. del Horno, J. Jover, M. Mena, A. Pérez-Redondo, C. Yélamos, *Angew. Chem. Int. Ed.* **2022**, *61*, e202204544; i) E. T. Ouellette, J. S. Magdalenski, R. G. Bergman, J. Arnold, *Inorg. Chem.* **2022**, *61*, 16064–16071.

[31] a) D. Sellmann, *Angew. Chem. Int. Ed. Engl.* **1972**, *11*, 534; b) B. Bayerl, K. Schmidt, M. Wahren, *Z. Für Chem.* **1975**, *15*, 277–278.

[32] Sutton and his group have later discovered that degradation of diazonium complexes can lead selectively to the analogous [(η^5-$CH_3C_5H_4$)$Mn(CO)_2(N_2)$] dinitrogen complex, but it was not isolated: a) C. Barrientos-Penna, D. Sutton, *J. Chem. Soc. Chem. Commun.* **1980**, 111–112; b) C. F. Barrientos-Penna, F. W. B. Einstein, D. Sutton, A. C. Willis, *Inorg. Chem.* **1980**, *19*, 2740–2749.

[33] Formation of Mn^I-N_2 complexes upon photolysis of carbonyl precursors has also been evidenced with time-resolved IR spectroscopy: a) J. A. Banister, M. W. George, S. Grubert, S. M. Howdle, M. Jobling, F. P. A. Johnson, S. L. Morrison, M. Poliakoff, U. Schubert, J. R. Westwell, *J. Organomet. Chem.* **1994**, *484*, 129–135; b) B. H. G. Swennenhuis, R. Poland, N. J. DeYonker, C. E. Webster, D. J. Darensbourg, A. A. Bengali, *Organometallics* **2011**, *30*, 3054–3063; c) J. B. Eastwood, L. A. Hammarback, M. T. McRobie, I. P. Clark, M. Towrie, I. J. S. Fairlamb, J. M. Lynam, *Dalton Trans.* **2020**, *49*, 5463–5470.

[34] I. Kulai, A. Karpus, L. Soroka, D. A. Valyaev, V. Bourdon, E. Manoury, R. Poli, M. Destarac, S. Mazières, *Polym. Chem.* **2018**, *10*, 267–277.

[35] After their initial preparation of [$CpMn(CO)_2(N_2)$] (**1**), Sellmann and co-workers have reported a method to purify it using HPLC at very low temperature. Because we had no access to an HPLC apparatus working under low temperatures, samples containing <10% cymantrene were used for the present study, without affecting the results. D. Sellmann, E. Jonk, H.-J. Reinecke, T. Würminghausen, *Fresenius Z. Für Anal. Chem.* **1979**, *294*, 372–374.

[36] a) K. Weidenhammer, W. A. Herrmann, M. L. Ziegler, *Z. Anorg. Allg. Chem.* **1979**, *457*, 183–188; b) W. A. Chomitz, J. Arnold, *Chem. Commun.* **2007**, 4797–4799; c) W. A. Chomitz, J. Arnold, *Dalton Trans.* **2009**, 1714–1720; d) D. C. Cummins, G. P. A. Yap, K. H. Theopold, *Eur. J. Inorg. Chem.* **2016**, 2349–2356.

[37] C. Perthuisot, M. Fan, W. D. Jones, *Organometallics* **1992**, *11*, 3622–3629.

[38] L. J. Farrugia, C. Evans, D. Lentz, M. Roemer, *J. Am. Chem. Soc.* **2009**, *131*, 1251–1268.

[39] A. O. Borissova, M. Y. Antipin, K. A. Lyssenko, *J. Phys. Chem. A* **2009**, *113*, 10845–10851.

[40] Such H-bond network can be found in other reported structures of cymantrene, see for example reference 38.

[41] M. Y. Darensbourg in *Progress in Inorganic Chemistry*, *Vol. 33* (Ed. S. J. Lippard), John Wiley & Sons, Inc., New York, **1985**, pp 221–274.

[42] E. O. Fischer, C. Apostolidis, E. Dornberger, A. C. Filippou, B. Kanellakopulos, B. Lungwitz, J. Müller, B. Powietzka, J. Rebizant, W. Roth, *Z. Naturforsch. B* **1995**, *2*, 1382–1395.

[43] H. J. Reich, D. P. Green, M. A. Medina, W. S. Goldenberg, B. Ö. Gudmundsson, R. R. Dykstra, N. H. Phillips, *J. Am. Chem. Soc.* **1998**, *120*, 7201–7210.

[44] IR monitoring of the reaction of PhLi·PMDTA with **1** in Et_2O revealed two close sets of CO stretches for **3**·PMDTA, suggesting that the Li^+ cation may interact with different moieties in the anionic Mn complex (see Figure S27).

[45] Two independent molecules of **3**·PMDTA are found in the unit cell, averaged metrical data are given.

[46] For representative examples of structurally characterized Mn(II) arylmanganate complexes, see: a) M. Uzelac, P. Mastropierro, M. de Tullio, I. Borilovic, M. Tarrés, A. R. Kennedy, G. Aromí, E. Hevia, *Angew. Chem. Int. Ed.* **2021**, *60*, 3247−3253; b) R. A. Musgrave, R. S. P. Turbervill, M. Irwin, J. M. Goicoechea, *Angew. Chem. Int. Ed.* **2012**, *51*, 10832−10835; c) R. A. Bartlett, M. M. Olmstead, P. P. Power, S. C. Shoner, *Organometallics* **1988**, *7*, 1801–1806.

[47] Deposition numbers 2246956 (for **1**), 2246957 (for **3**·PMDTA), 2246958 (for **4**·PMDTA), and 2246958 (for **2**·PMDTA) contain the supplementary crystallographic data for this paper. These data are provided free of charge by the joint Cambridge Crystallographic Data Centre and Fachinformationszentrum Karlsruhe Access Structures service.

[48] W. T. Boese, B. Lee, D. W. Ryba, S. T. Belt, P. C. Ford, *Organometallics* **1993**, *12*, 4739–4741.

[49] Intriguingly, the same temperature sensitivity was observed by Sellmann in the reaction of **1** with methyllithium that leads above –20 °C to the methylate complex [$Cp(CO)_2MnMe$]Li. The CO stretching frequencies of the latter were reported to be very close to the presumed methyldiazenido complex. See: D. Sellmann, P. Klostermann, *Z. Naturforsch. B* **1983**, *38B*, 1497–1500.

[50] A. P. Scott, L. Radom, *J. Phys. Chem.* **1996**, *100*, 16502–16513.

[51] Functionalization of the proximal (α) nitrogen of an end-on dinitrogen ligand triggered by electrophilic attack at the distal (β) nitrogen is known, see: M. M. Deegan, J. C. Peters, *Chem. Sci.* **2018**, *9*, 6264–6270 and references 9 and 23e.